Electronic Supplementary Information

# Achieving Current Rectification Ratio ≥ $10^5$ across Thin Film of Coordination Polymer

Anupam Prasoon, Barun Dhara, Debashree Roy, Shammi Rana, Sujit Bhand and Nirmalya Ballav*

*Department of Chemistry, Indian Institute of Science Education and Research (IISER) Pune, Dr. Homi Bhabha Road, Pashan, Pune – 411 008, Maharashtra, India*

Corresponding Author: nballav@iiserpune.ac.in

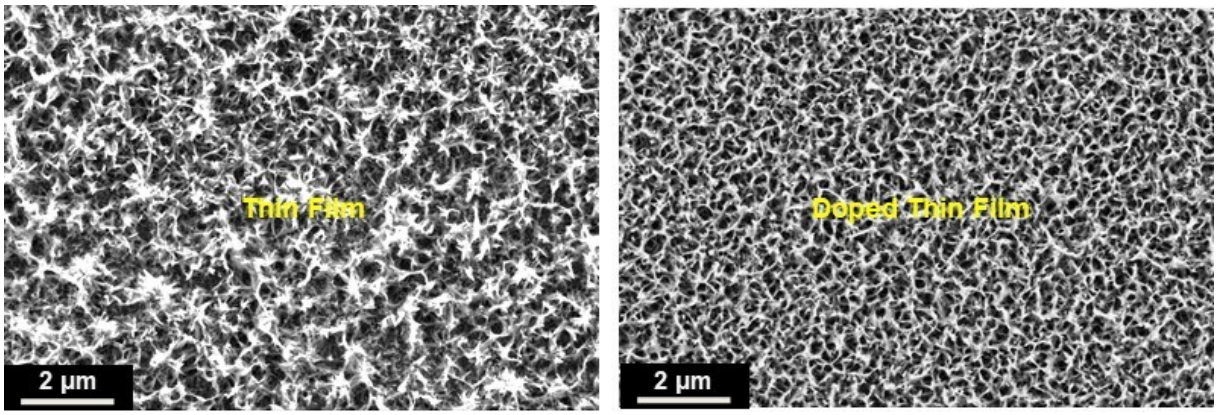


**Figure S1.** Zoomed-in FE-SEM images on pristine Cu-BTEC (left) and doped Cu-BTEC (right) thin films.

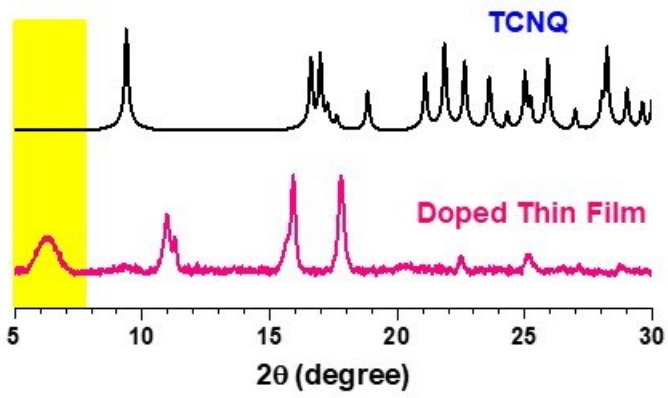


**Figure S2.** PXRD patterns of bulk TCNQ (black) and TCNQ doped Cu-BTEC thin film (pink).

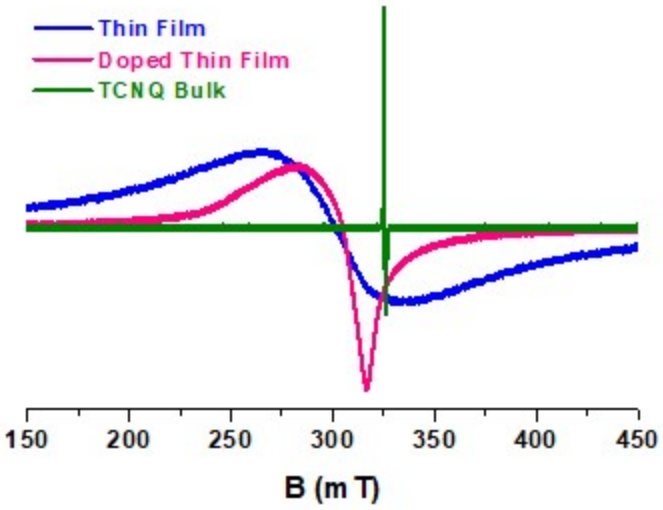


**Figure S3.** EPR spectra recorded on pristine Cu-BTEC thin film (blue), TCNQ doped Cu-BTEC thin film (pink) and TCNQ bulk powder (green).

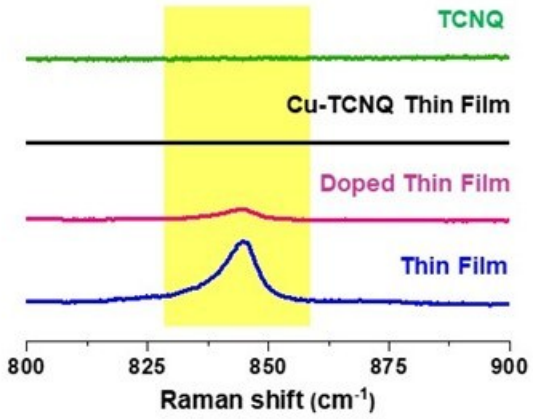


**Figure S4.** Raman spectra of pristine and doped Cu-BTEC thin films and pristine Cu-TCNQ thin film. Band characteristic of C-H out-of-plane bending mode at ~845 $cm^{-1}$ (highlighted in yellow) in the doped Cu-BTEC thin film is suppressed in comparison to pristine Cu-BTEC thin film which was absent in pristine Cu-TCNQ thin film.

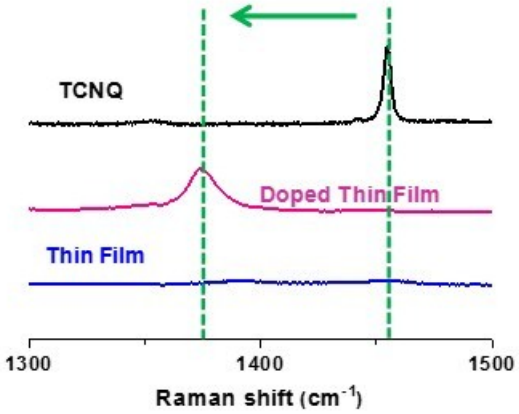


**Figure S5.** Raman spectra of pristine (blue) and doped Cu-BTEC (pink) thin films and of pure TCNQ (black). A significant red-shift of the band characteristic of C=C wing stretching mode of TCNQ from ~1455 $cm^{-1}$ to ~1374 $cm^{-1}$ was observed in doped thin film (pink).

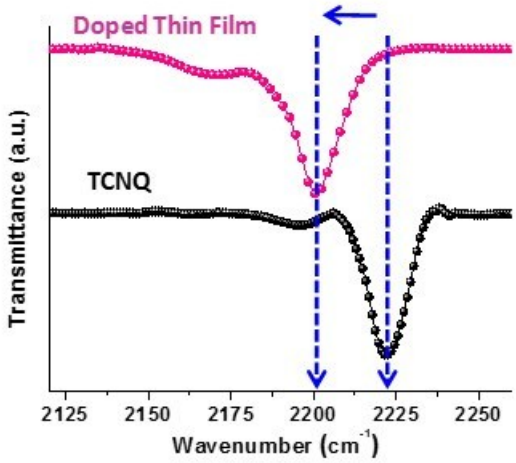


**Figure S6.** FTIR spectrum of pure TCNQ (black) and IRRAS spectrum of doped Cu-BTEC thin film.

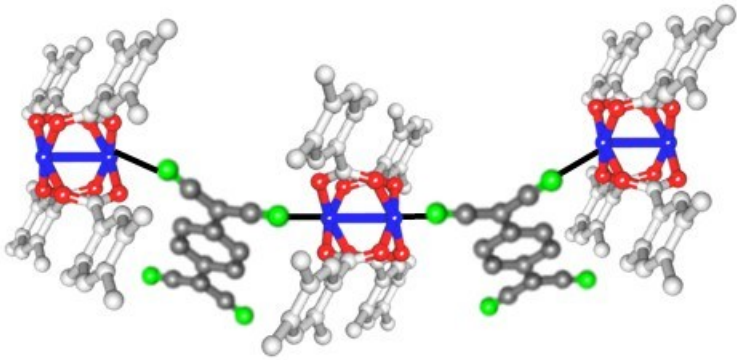

**Figure S7.** Schematic of bonding motif of TCNQ molecules to Cu-BTEC units.

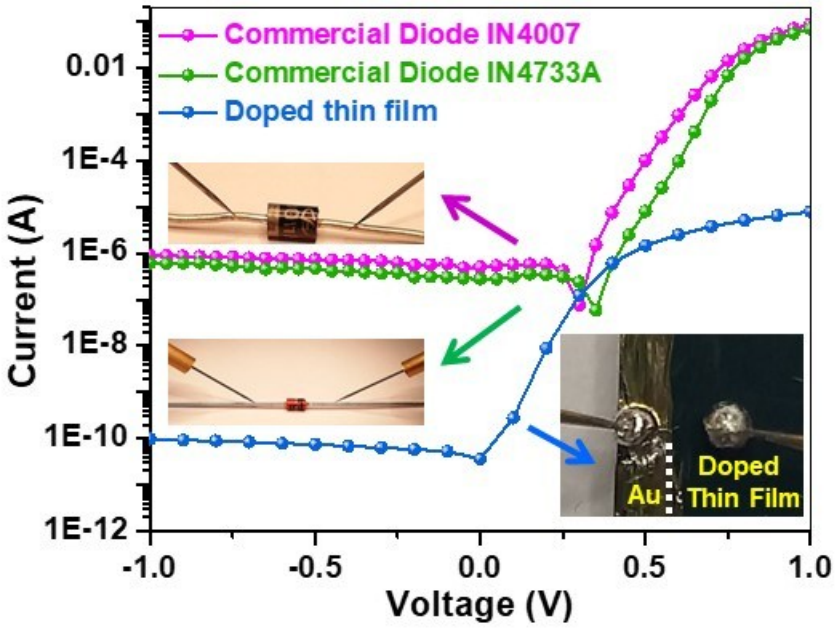


**Figure S8.** Direct comparison of I-V characteristics of the doped Cu-BTEC thin film (blue) with commercial Si rectifier diodes (1N4007, magenta and 1N4733A, green; and respective optical images are shown). An optical image of TCNQ doped Cu-BTEC thin film device showing the cross-plane I-V measurement after scratching out sample to expose the Au substrate.

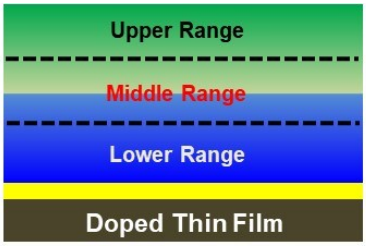


| Upper Range (Nitrogen) | Middle Range (Nitrogen) | Lower Range (Nitrogen) |
|---|---|---|
| 23.49 (a) | 14.89 (d) | 3.87 (g) |
| 26.62 (b) | 15.62 (e) | 1.85 (h) |
| 18.95 (c) | 11.50 (f) | 3.65 (i) |

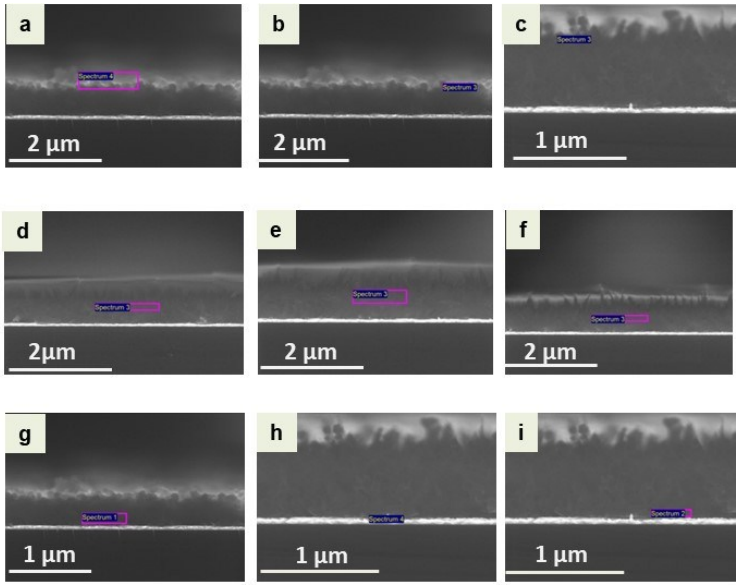


**Figure S9.** Cross-sectional EDXS analysis of the doped Cu-BTEC thin film in three different ranges (upper, middle and lower) with corresponding FE-SEM images.

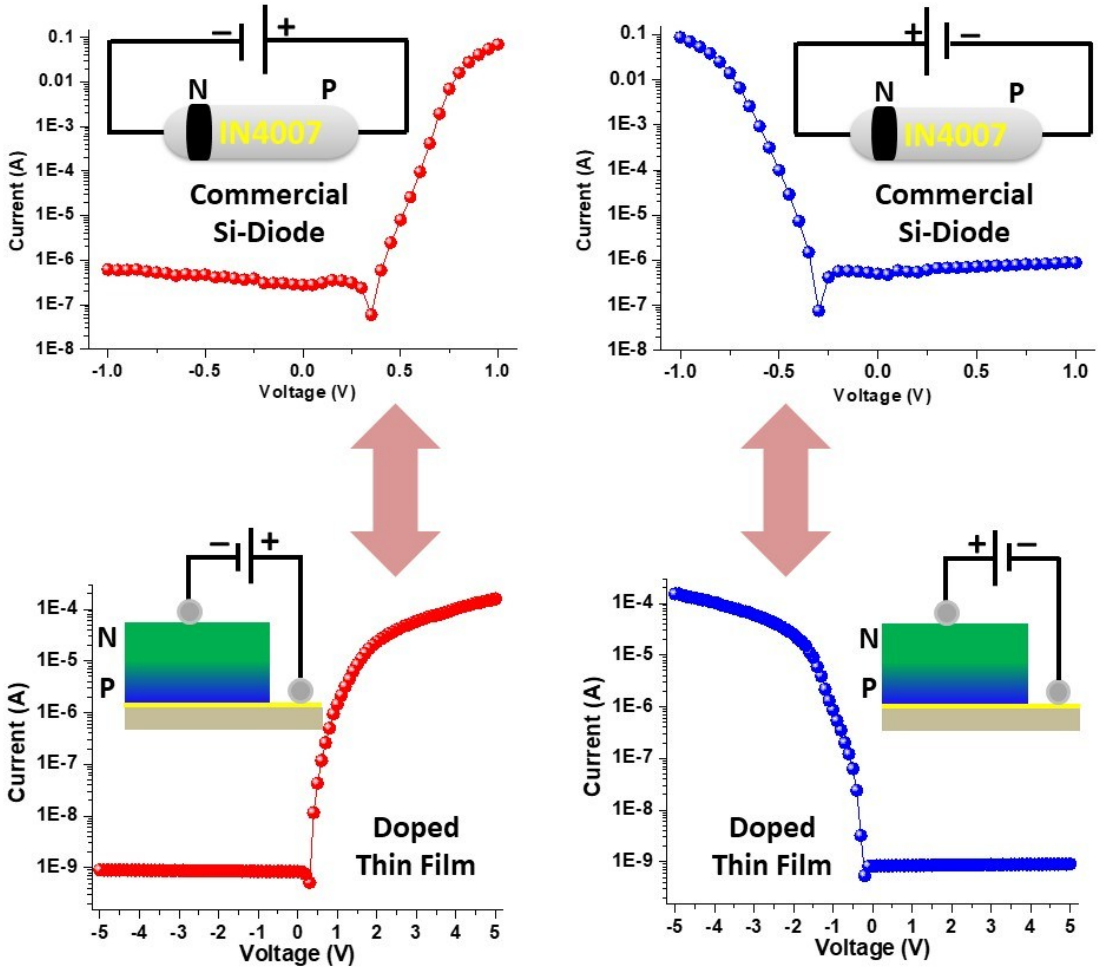


**Figure S10.** I-V characteristics on commercial IN4007 Si diode in forward bias (top left, red circles) and reverse bias (top right, blue circles). I-V characteristics of our TCNQ doped Cu-BTEC thin film upon changing the direction of current flow from SMU-2 to SMU-1 (bottom left, red circles, forward bias) and SMU-1 to SMU-2 (bottom right, blue circles, reverse bias). Identities of p and n sides are marked for clarity.

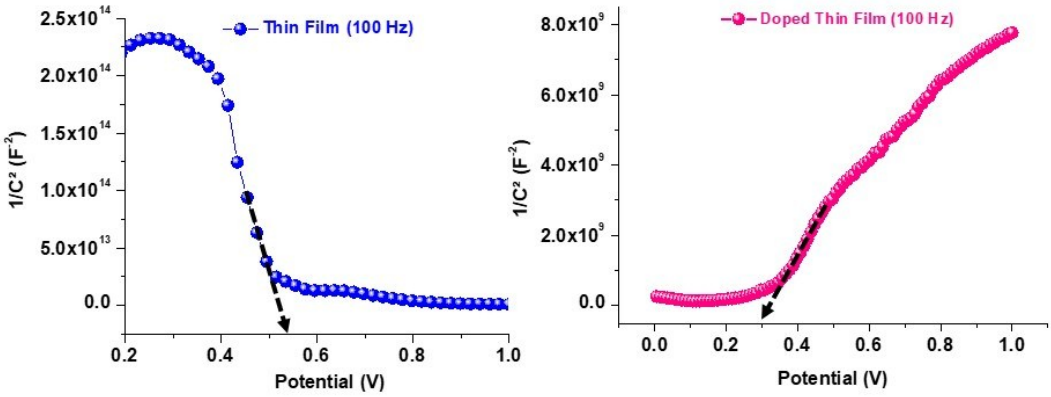


**Figure S11:** Mott-Schottky plots ($1/C^2$ versus V where C is capacitance and V is voltage) recorded on pristine (left panel) and doped (right panel) Cu-BTEC thin films at 100 Hz. Respective slopes are indicated by black arrows.

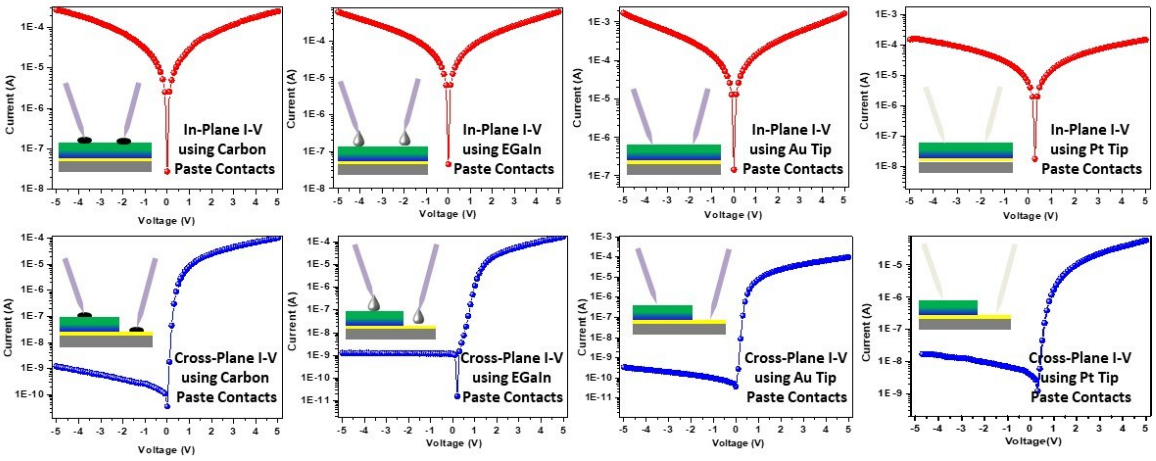


**Figure S12.** I-V characteristics of the doped Cu-BTEC thin film both in-plane (top panels) and cross-plane (bottom panels) modes recorded using various contacts (C-paste, EGaIn, direct Au-tip and direct Pt-tip).

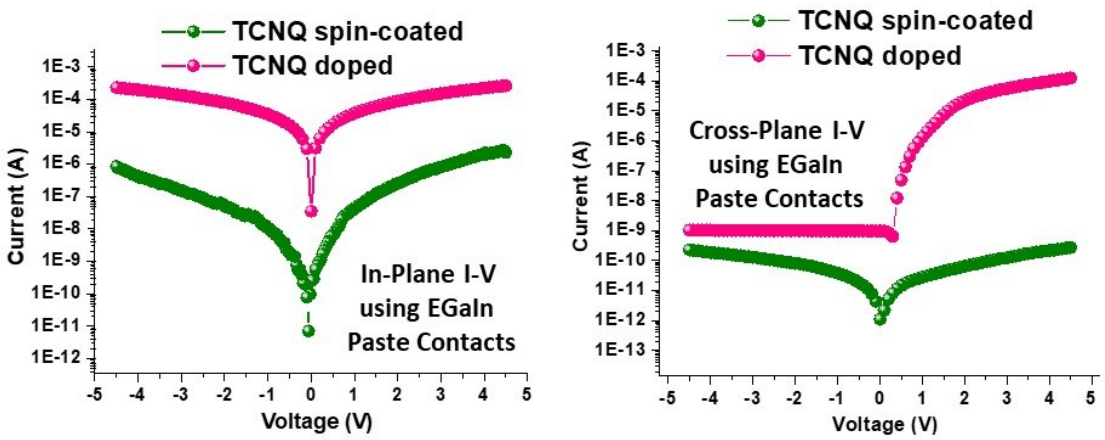


**Figure S13.** I-V characteristics recorded on the TCNQ spin-coated Cu-BTEC thin film both in-plane (left) and cross-plane (right) modes using EGaIn contacts (green circles). As reference, data on TCNQ doped Cu-BTEC thin film are provided (pink circles) and the marked difference is the current rectification.

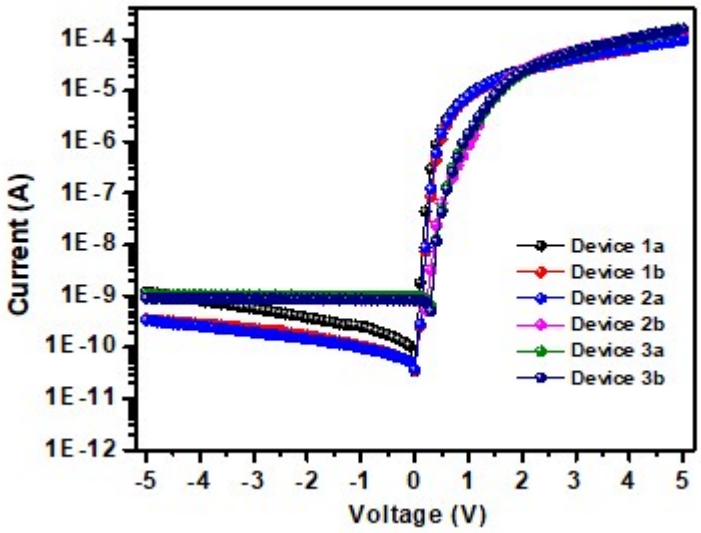


**Figure S14.** Cross-plane I-V characteristics on 3 different batches of TCNQ doped Cu-BTEC thin film and on two different points on the sample surface.

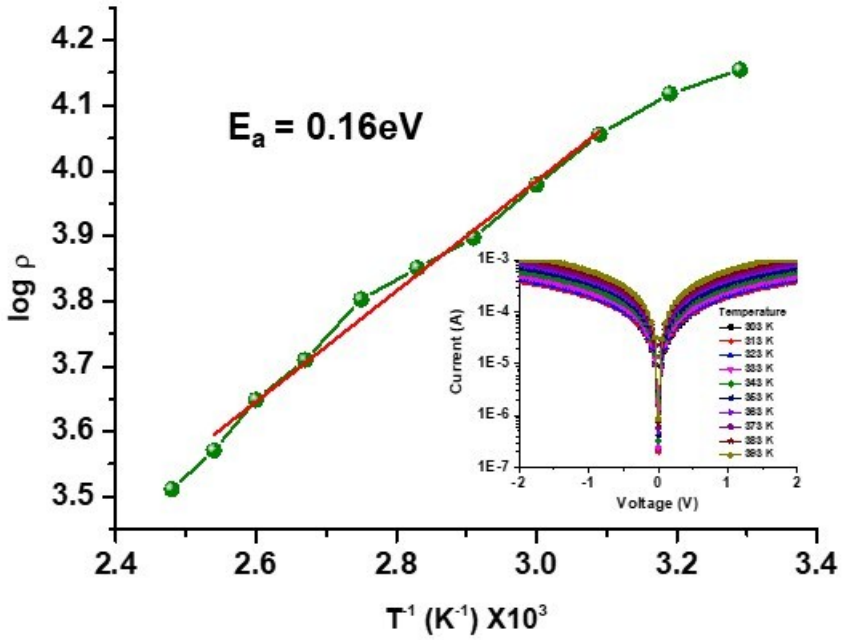


**Figure S15.** Estimation of activation energy ($E_a$) from Arrhenius plot extracted from the temperature-dependent conductance study.

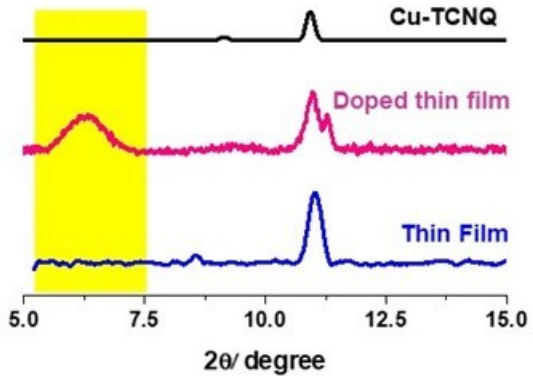


**Figure S16.** Out-of-plane XRD pattern of pristine (blue) and doped (pink) Cu-BTEC thin films and of pristine Cu-TCNQ thin film. The peak at $2\theta$~$5.8^0$ characteristic of pore-filling phenomenon in Cu-BTEC system is not a characteristic of pristine Cu-TCNQ thin film (highlighted in yellow).

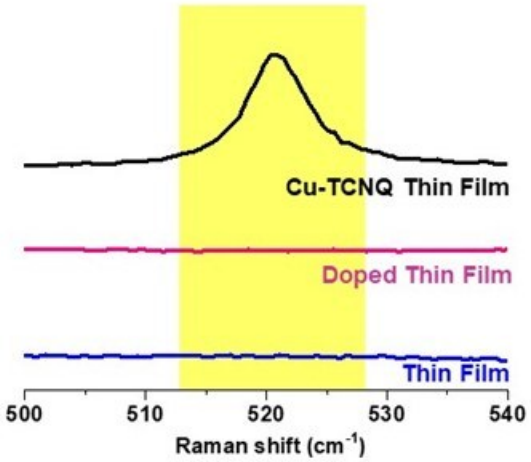


**Figure S17.** Raman spectra of pristine (blue) and doped (pink) Cu-BTEC thin films and of pristine Cu-TCNQ thin film (black). Band at 520 $cm^{-1}$ is due to Cu---Cu interaction mode appeared in pristine Cu-TCNQ thin film was consistently absent in both pristine and doped Cu-BTEC thin films (highlighted in yellow).

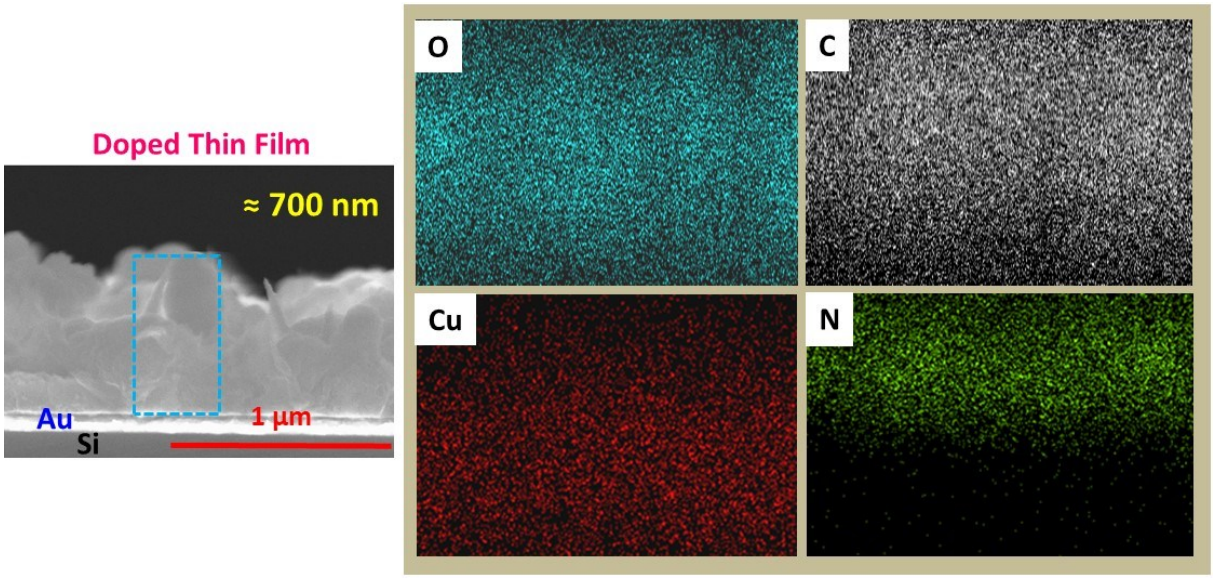


**Figure S18.** Cross-sectional elemental mapping of O, C, Cu and N on the doped Cu-BTEC thin film by EDXS analysis showing the absence of TCNQ in lower region near the Au substrate.

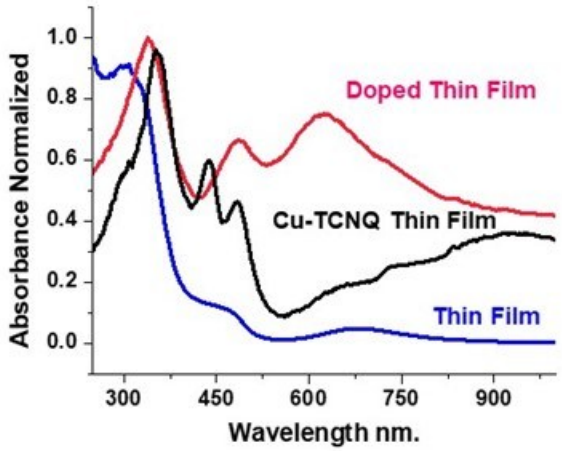


**Figure S19.** Distinctive solid-state UV-vis spectra of pristine (blue) and doped (pink) Cu-BTEC thin films and of pristine Cu-TCNQ thin film (black).

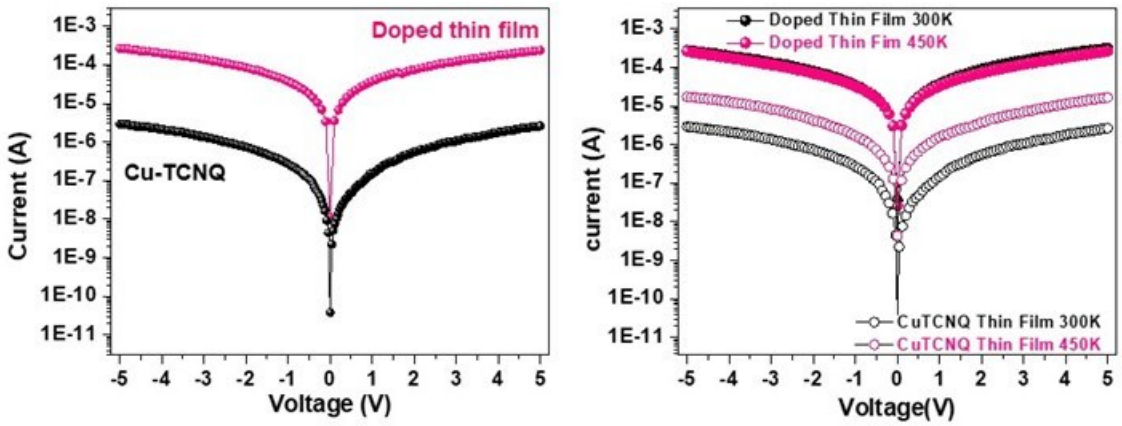


**Figure S20.** In-plane I–V characteristics of doped (pink) Cu-BTEC and pristine Cu-TCNQ (black) thin films (left panel). Variable-temperature in-plane I-V characteristics of doped Cu-BTEC thin film recorded at 300 K (black filled circle) and at 450 K (pink filled circle); and of pristine Cu-TCNQ thin film recorded at 300 K (black open circle) and at 450 K (pink open circle) (right panel).